Original Research Article

DFT and monte carlo simulation for the prediction of corrosion inhibitive efficacy of selected thiosemicarbazide derivatives on Al (111) and Cu (111) surfaces in acidic media

Terngu Timothy Uzah* 🔴

*Department of Chemistry, College of Science, Federal University of Petroleum Resources, Effurum, Nigeria*

ARTICLE INFORMATION

ABSTRACT

The manufacturing industries are very concerned about corrosion. To cut expenses and preserve lives, corrosion control is still crucial. Using the density functional theory (DFT) method and Monte Carlo simulation, the anti-corrosion potentials of specific derivatives of thiosemicarbazide were studied. The energy gaps, highest occupied molecular orbital energy, lowest unoccupied molecular orbital energy, global softness, number of transferred electrons, and other reactivity characteristics were calculated at the B3LYP/6-31G+ (d.p) level of theory. Electrostatic potential (ESP) surface analysis was used to identify the reactive areas. MC simulation was used to study the compounds' adsorption behavior on the Al (111) and Cu (111) surfaces in an acidic solution. The compounds had low ΔE, E_{LUMO}, I, and η and high E_{HOMO}, A, σ, and ΔN, which explained their corrosion inhibition potentials. This is due to their shown capacity, as demonstrated by the ESP surface analysis, to both accept and donate electrons via back-donation to the metal's d-orbital. The MC simulation demonstrated a favorable contact between the inhibitory compounds and the surfaces of Al (111) and Cu (111) in the acidic medium. In the manufacturing sectors, these substances may be employed as corrosion inhibitors.

Corresponding author, email: uzah2t@gmail.com (T.T. Uzah).

Graphical Abstract
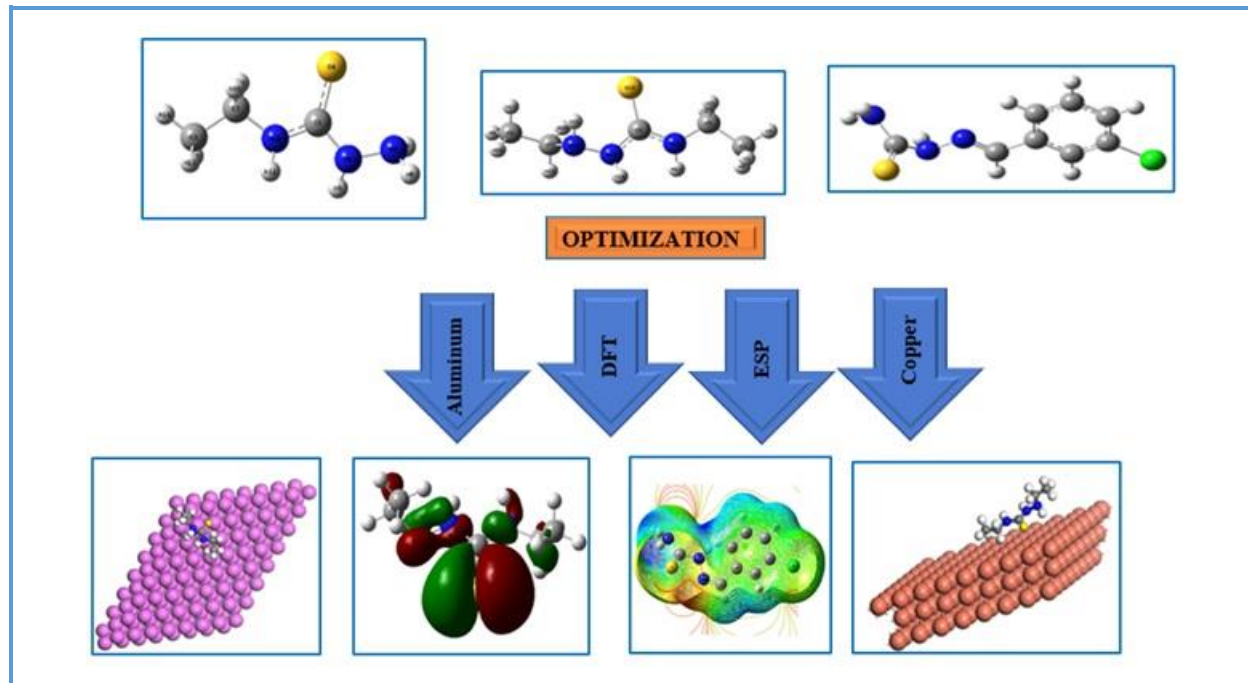
Introduction

The special mechanical strength and electrical conductivity of metals make them useful in the chemical, automotive, aerospace, and marine industries. Since they are so pure, they are also utilized in electronics as anodic materials for high-energy-density power sources [1-3]. Metals are coated with a protective layer called passivating oxide, which is sticky, but it also has an amphoteric susceptibility, which makes the metal easily dissolve in concentrated acidic and basic solutions with pH values between 4 and 9 [4,5]. The primary goal in reducing the electrochemical corrosion of metals is to separate the metal from corrosive substances. This can be accomplished by either forming a more resistant oxide film on the metal surface or by employing corrosion inhibitors, which stop the aggressive anions from adhering to the metal [6]. Consequently, several research projects have been undertaken to create organic inhibitors that are low-toxic, inexpensive, biodegradable, ecologically friendly, and safe to use with a wide enough safety margin. Many collaborative research papers on substituting novel ecologically suitable inhibitors for toxic compounds have been published in recent years [7-9] Because electronegative functional groups like the electronegative nitrogen, sulfur, and oxygen atoms, and p-electrons in triple or conjugated double bonds are often good inhibitors, the existence of these groups in organic components makes them important as inhibitors [10].

The precise interaction between the functional groups and the metal surface determines the effectiveness of suitable inhibitors, which is why these elements and sites are crucial. [11] Several investigations show that thiosemicarbazide derivatives are efficient corrosion inhibitors for several metals, including mild steel, copper and its

alloys, aluminum, and zinc in acidic conditions, however, only a small number of these compounds have been documented [12-15].
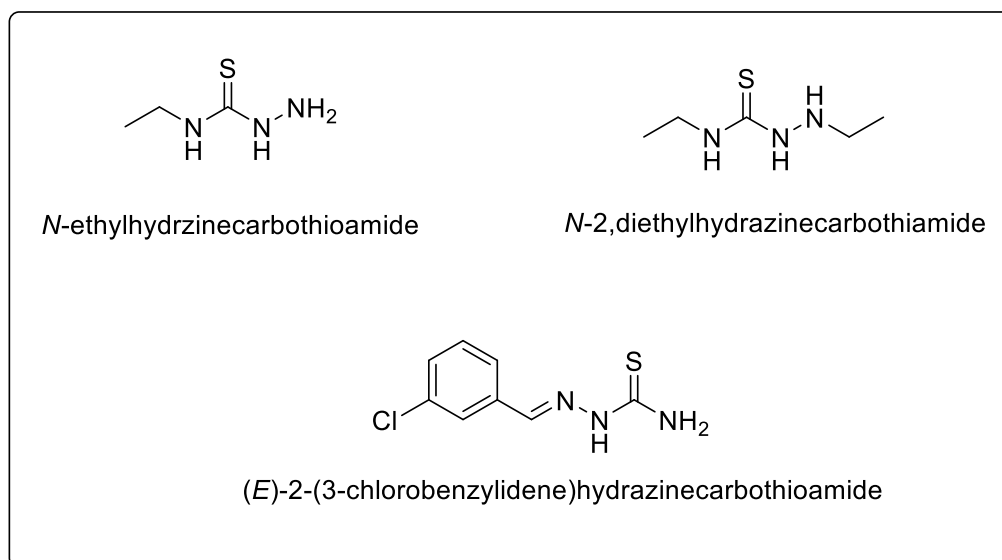
The purpose of this work was to examine, theoretically, the suppression of copper and aluminum corrosion in an acidic media using three organic molecules that are derivatives of thiosemicarbazide and are environmentally benign. Using Gaussian software and density functional theory (DFT), three thiosemicarbazide derivatives, namely N-ethylhydrazinecarbothioamide (compound A), N,2-diethylhydrazinecarbothioamide (Compound B), and (E)-2-(3-chlorobenzylidene) hydrazinecarbothioamide (Compound C), were primarily used as inhibitors of copper and aluminum alloy in an acidic medium. This is a relatively uncommon occurrence in the literature. In addition, utilizing Monte Carlo simulations, the inhibitor adsorption mechanism was examined and analyzed.

Computational Details

Density functional Theory (DFT) calculations

Quantum chemical calculations were performed on the isolated molecules using Becke's three -Lee–Yang–Parr correlation functional level (B3LYP) with the 6-311G+ (d,p) basis sets for a good balance between computation and accuracy, the B3LYP functional technique is recommended and 6-311G+ (d, p) basic set for N, C, S, and H atoms' modeling chemistry [16,17] implemented in Gaussian 09W software.

The isolated molecule has undergone thorough geometry optimization [18] using the universal solvation model. At this point, frequency calculations are made to ascertain the properties of the stationary spots. In this case, several descriptors related to quantum chemistry were produced. Computing the energy of the highest occupied molecular orbital (E_{HOMO}), the lowest unoccupied molecular orbital (E_{LUMO}), global softness (σ), chemical hardness (η), and fractions of electrons transferred (ΔN), ionization potential (I), electron affinity (A), and ESP maps were among their distinctive characteristics.

N-ethylhydrzinecarbothioamide

N-2,diethylhydrazinecarbothiamide

(*E*)-2-(3-chlorobenzylidene)hydrazinecarbothioamide

Figure 1. Molecular structure of the thiosemicarbazide derivatives (Compounds A-C).

$$A = E_{LUMO} \qquad (1)$$

$$I = E_{HOMO} \qquad (2)$$

$$\Delta E = E_{LUMO} - E_{HOMO} \qquad (3)$$

$$\eta = \left(\frac{\delta^2 E}{\delta N^2}\right)_v = \left(\frac{\delta \mu}{\delta N}\right)_v = \frac{\Delta E}{2} \qquad (4)$$

$$\sigma = 2\left(\frac{\delta N}{\delta \mu}\right)_{v(r)} = \frac{1}{\eta} = \frac{2}{\Delta E} \qquad (5)$$

$$\chi = \frac{-(E_{HOMO} + E_{LUMO})}{2} \qquad (6)$$

$$\Delta N = \frac{(\chi_{metal} - \chi_{inh})}{2 \times (\eta_{metal} - \eta_{inh})} \qquad (7)$$

Where,

Electron affinity (A), Ionization Potential (I), E_{HOMO} = The highest occupied molecular orbital's energy, E_{LUMO} = The lowest unoccupied molecular orbital, ΔE = energy gap, χ = global electronegativity, σ = global softness, η = chemical hardness and ΔN = fractions of electrons transferred, χ_{meta} (χ_{Cu} = 4.94 eV χ_{Al} = 4.26 eV) and χ_{inh} = absolute electronegativities of the metal and organic inhibitor respectively. η_{metal} (η_{Cu} = η_{Al} = 0 eV) and η_{inh} = absolute hardness of the metal and organic inhibitor, respectively [17].

Monte carlo simulation

Cu (111) and Al (111) were used as standard metal surfaces in the MC simulation to study the adsorption progress of the molecules. This was made possible based on previous studies [19,20], which are sufficient when looking for surfaces with a well-packed structure and good stability [20]. Forcite was used to optimize compounds (A-C), and a model of the metal surface (8 x 8) supercell; vacuum thickness (30); box volume (6) was created. Fine-quality adsorption was calculated using five annealing cycles with 5000 steps per cycle [18]. To simulate a real-world environment, the MC simulation was run on optimized low-energy Cu (111) and Al (111) utilizing water and acidic media. Using an adsorption locator module with a COMPASS forcefield, the molecules were adsorbed on Cu

(111) and Al (111) surfaces. An estimate of the adsorption energy was made [6,22]. A number of significant parameters were determined from the MC simulation, including the total energy of the system [E_{total}], Deformation energy [E_{def}], Rigid adsorption energy [E_{rigid}], Adsorption energy [E_{ads}], and Metal adsorbate configuration energy [dE_{ads}/dN_i] of molecules. The total of the deformation energy (E_{def}) and rigid adsorption energy (E_{rigid}) is often known as adsorption energy (E_{ads}) [18]:

Results and Discussion

Density functional theory (DFT) analysis

The DFT/B3LYP/6-311 G+ optimized structures of the three thiosemicarbazide derivatives are seen in Figure 2. Electron affinity (A), Ionization Potential (I), global softness (σ), global electronegativity (χ), chemical hardness (η), Energy gap (ΔE), and electron transfer (ΔN) are some of the suggested quantum descriptors that could be in charge of the studied molecules' effective inhibition (Table 1).

The energy gap (ΔE)

The ΔE is the difference between a molecule's E_{LUMO} and E_{HOMO}, and it connects the inhibitor's reactivity to adsorption on the metal surface. Reduce the ΔE value of inhibitors to enhance the reactivity between the metal and the inhibiting molecule, hence increasing the metal's surface binding capability. Due to the decreased energy needed to remove the electron from the highest occupied molecular orbital, this increase in binding capacity may result in a rise in the inhibitor's inhibitory efficiency [21]. The destabilization of the highest unoccupied molecular orbital to a lower energy level may be the cause of the extremely low band gap of

0.1513 eV observed for Compound C when the phenyl group was attached. According to Table 1 ΔE value, indicates that these molecules perform better than others due to their lower energy gaps and stronger reactivity as follows; Compound C > Compound A > Compound B.

The energy of the highest occupied molecular orbital (E_{HOMO}) or electron affinity (A)

The electron donor capacity of an inhibitor is linked to its E_{HOMO}. Inhibitors with high or increased E_{HOMO} have a greater propensity to transfer electrons to the metal's corresponding lower molecular orbital. As a result, inhibitors have a greater ability to adsorb onto metal surfaces and to inhibit them effectively. Therefore, by improving the transferring process, an inhibitor's effectiveness can be increased. Table 1 clearly illustrates how Compound A > Compound B > Compound C corresponds to the E_{HOMO} values for the three thiosemicarbazide derivative molecules. The greatest inhibitor of electron donation to the metal's vacant d-orbital is Compound A, which has the largest E_{HOMO} (-0.2026 eV). In contrast, organic inhibitors both take electrons from the metal's d-orbital and give them to its empty d orbitals [22].

The lowest unoccupied molecular orbital (E_{LUMO}) or ionization potential (I)

It is clear from E_{LUMO} that an inhibitor can take up electrons from the metal, which would enhance the inhibitory impact on the metal's surface. This could account for the potential of the inhibitor molecules interacting (adsorbing) through their acceptor atoms on the metallic surface, which frequently have a positive charge as previously noted [23,24]. Compound B > Compound A > Compound C E_{LUMO} sequence suggests that Compound B has a higher inclination to take electrons from a metal's surface. Electrons are focused on the atoms of the phenyl group and the molecular structure of the molecules under study, according to the analysis of the electron density distribution in molecular orbitals (Figure 3) [25,26].

Global softness (σ) and *chemical hardness (η)*

According to the acid and base theory, which established that molecular hardness is equal to the geometric mean of the chemical hardness of its component atoms [12,27], absolute hardness and softness reactivity descriptors are linked to the description of soft and hard solutions. Every chemical reaction involves the transfer of electrons between different chemical species; charge transfer affects soft molecules differently than it does hard molecules. Chemical stability and hardness are directly related, according to the Principle of Maximum Hardness [28], which also argues that harder molecules are less reactive and more stable. Therefore, the resistance of the electron cloud of ions, atoms, or molecules to polarization or deformation brought on by disturbances in chemical reactions is indicated by a molecule's chemical hardness. A reaction's chemical hardness provides essential information for forecasting the reaction mechanism and estimating the products produced throughout the reaction [12]. The sequence of values for absolute hardness is as follows: Compound C < Compound A < Compound B. This makes these three molecules more reactive and less stable. Low bandgap derivatives have strong inhibitory efficiency because of their low hardness values. The commonly accepted belief that hard molecules should have a large energy gap and soft molecules should have a small energy gap is supported by this. The sequence of the molecules that were

investigated using DFT and their softness values is as follows: Compound B < Compound A < Compound C. Therefore, a low global hardness value, or a high global softness value, is probably going to exhibit a high inhibitory efficiency.

Global electronegativity (χ)

Electronegativity, the atom's propensity to draw a shared pair of electrons to itself within a molecule, is a fundamental idea in comprehending the nature of chemical interactions. When a molecule forms, the electronegativities of its constituent atoms are brought into equilibrium, and the resultant quantity known as molecular electronegativity is the geometric mean of those electronegativities [12,29]. The electronegativity values of the molecules under study are as follows (Table 1): Compound A < Compound B < Compound C.

Number of electrons transferred (ΔN)

The quantity of electrons moved from the inhibiting molecule to the metal's surface is known as the proportion of electrons transferred (ΔN). It also displays the electron-transfer capacity of the inhibitor. An inhibitor's ability to donate electrons increases along with its inhibitory efficiency on the metal surface. Similarly, when there are more electron transfers, an inhibitor's efficiency rises on the metal surface. For an organic inhibitor to be considered efficient in enhancing the corrosion inhibition efficiency, its number of electrons transferred (ΔN) must be fewer than 3.6 (electrons). If the ΔN is more than 3.6 (electrons), the inhibition efficiency will drop [30]. Higher electron transfer value molecules are more likely to give electrons to the other molecules that are receiving them. This suggests that inhibitory compounds with larger ΔN have a higher propensity to adsorb on the metal surface, increasing their inhibition efficiency as a result [31]. The order in which the number of electrons transferred for copper (ΔN_{Cu}) and the number of electrons transferred for aluminum (ΔN_{Al}) grows for molecules under study is as follows: Compound C > Compound A > Compound B. The substituent group and molecular structure of thiosemicarbazide skeleton ring have a significant impact on the ΔN values. This finding indicates that although the copper and aluminum surfaces may be electron-accepting molecules, the investigated thiosemicarbazide derivatives are electron-donating molecules.

Compound A

Compound B
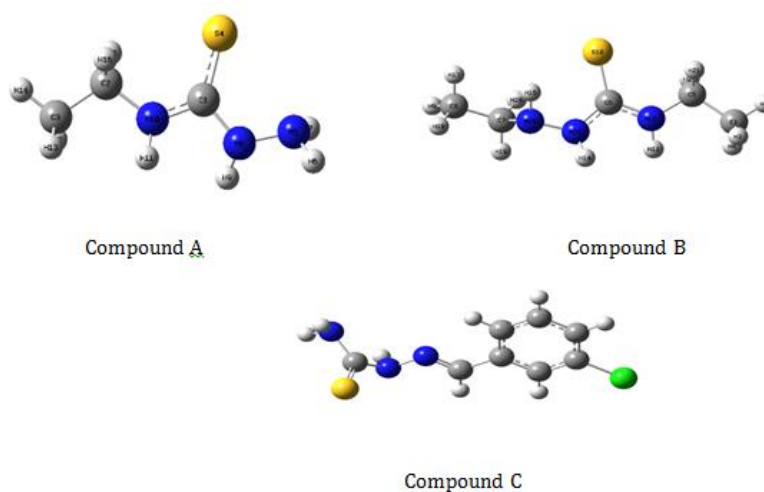
Compound C

Figure 2. Optimized structures of the thiosemicarbazide derivatives (Compounds A-C).
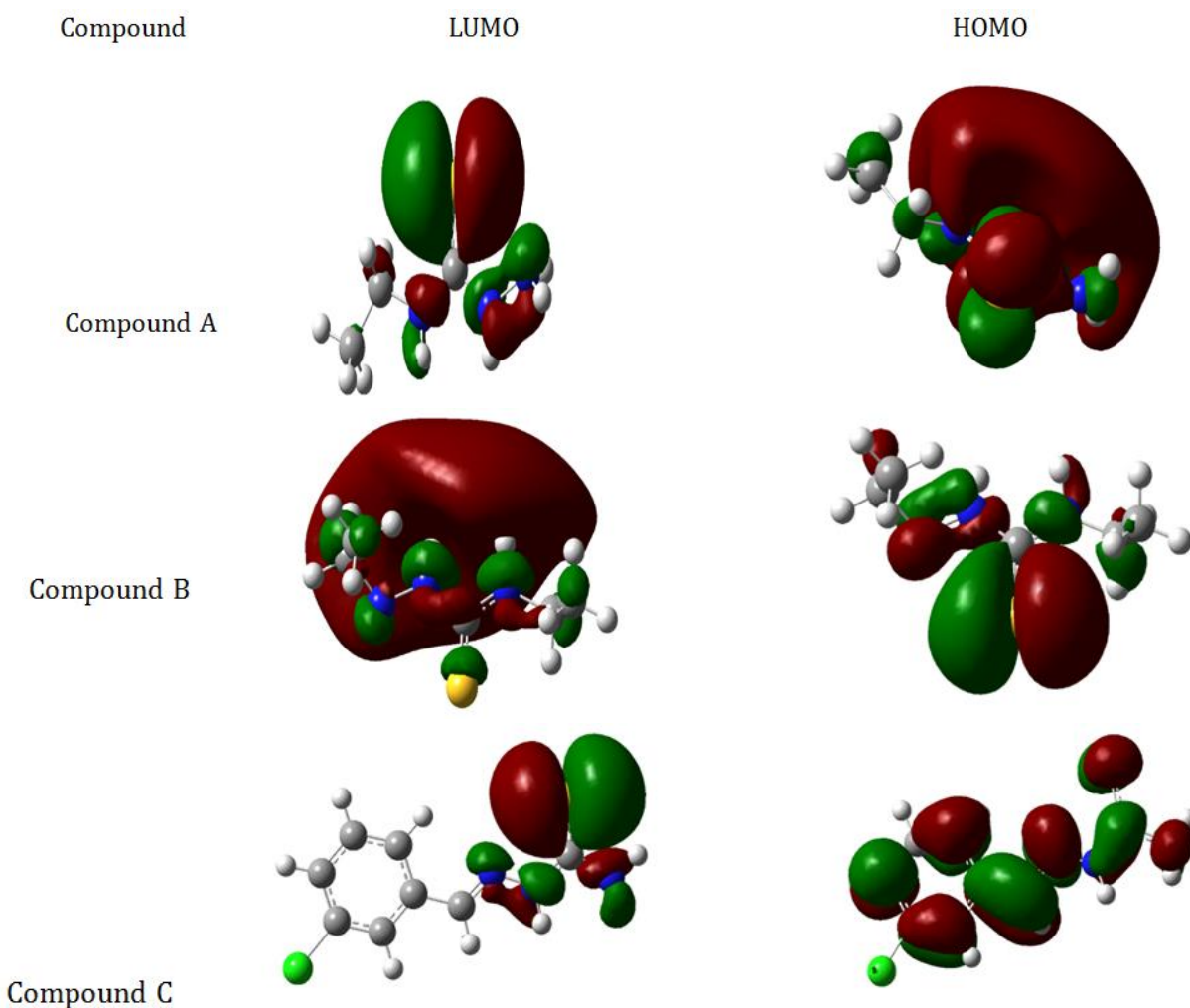
**Figure 3.** LUMO (left) and HOMO (right) structures of the thiosemicarbazide derivatives (compounds A-C).

Table 1. The evaluated quantum chemical parameters for the compounds (eV)

Compound	E_{LUMO}	E_{HOMO}	ΔE	η	σ	χ	ΔN_{Al}	ΔN_{Cu}
A	-0.0185	-0.2026	0.1841	0.0921	10.86	0.111	-16.93	-26.22
B	-0.0183	-0.2177	0.1994	0.0997	10.03	0.1180	-15.61	-24.18
C	-0.0704	-0.2217	0.1513	0.0757	13.22	0.146	-20.37	-31.66

Electrostatic potential maps (ESP)

The electron-rich and electron-deficient regions of molecules are better understood with the aid of the ESP maps [32]. The sites that promote an electrophilic assault are represented by the red and orange areas (negative portions) of the map, whereas the blue and green regions (positive parts) of the map represent the sites that favor a nucleophilic attack (Figure 4). The nitrogen, sulfur, and phenyl hydrogen atoms prefer a nucleophilic attack while an electrophilic attack is favored by some carbon and phenyl carbons.

Compound   ESP Map   Surface contour

Compound A

Compound B
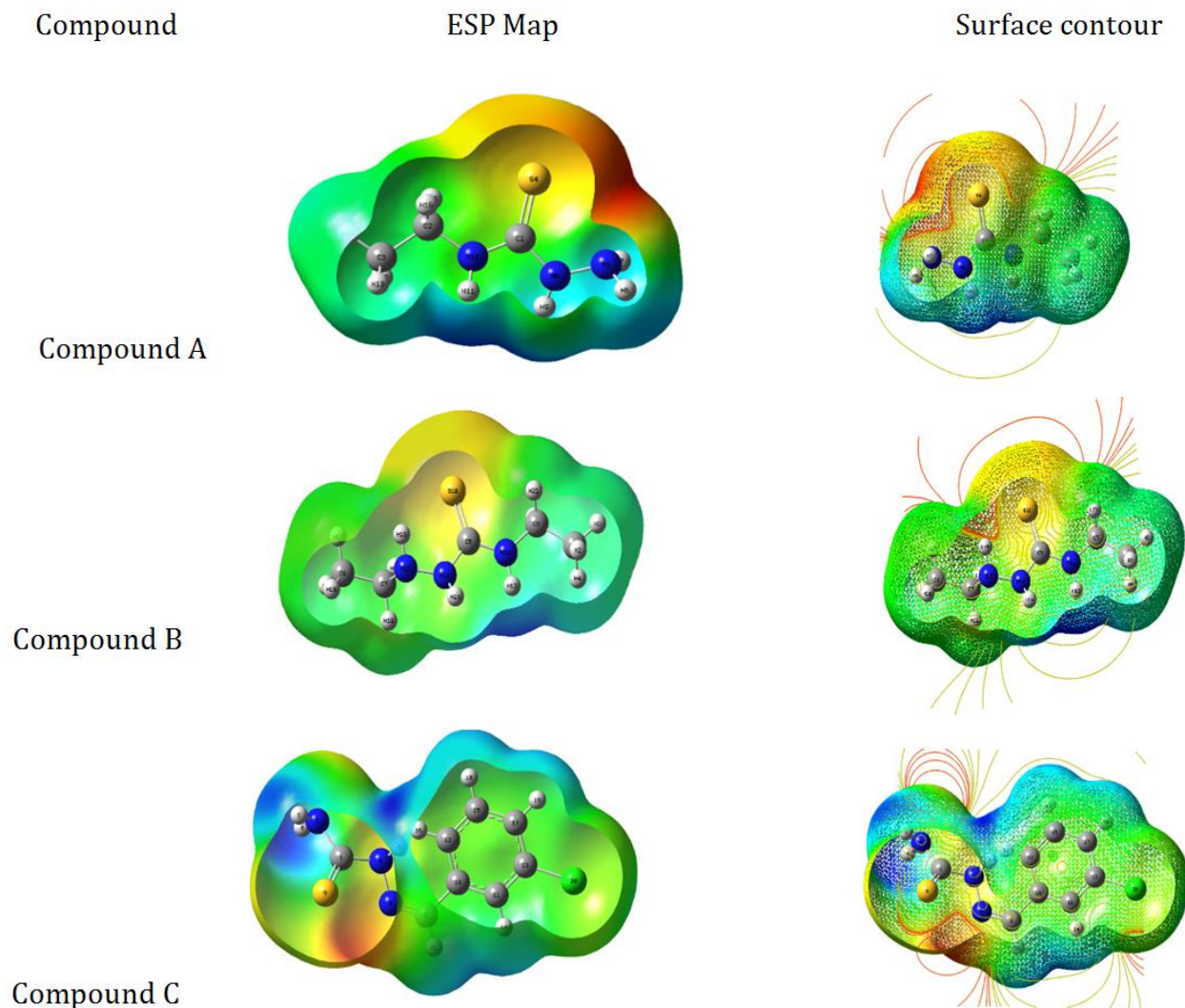
Compound C

Figure 4. Electrostatic potential map (left) and surface contour (right) of the thiosemicarbazide derivatives (Compounds A-C).

Monte Carlo simulation

The compounds under examination on Cu (111) and Al (111) surfaces are demonstrated in Figures 5 and 6. While Tables 2 and 3 list their total energy (E_{Tot}), adsorption energy (E_{Ads}), rigid adsorption energy (E_{Rigid}), and deformation energy (E_{Def}). The compounds' E_{Tots} are as follows: Compound C > Compound A > Compound B. The compound's adsorption on the metal surfaces is thermodynamically stabilized, as indicated by all values, with Compound C being the best. One adsorbate component removed from a metal adsorbate configuration is often represented by the energy of the substrate-adsorbate configuration (dE_{ads}/dN_i). Generally speaking, the greater the inhibitor-metal component interaction, the lower the value of dE_{ads}/dN_i. In addition, it has typically been discovered that adsorption efficiency increases with addition substituents, such as functional groups found in inhibitor compounds, adsorption energy, and the dE_{ads}/dN_i value [18,33]. Compound C > Compound A > Compound B is the order of the dE_{ads}/dN_i. The compounds may be able to stop

or slow down corrosion because they also have low adsorption energies. The order of the E_{Ads} is Compound C > Compound A > Compound B. E_{Rigid} plus E_{Def} add up to E_{Ads}. Whereas the energy released on Cu (111) and Al (111) when the unrelaxed adsorbate components are adsorbed is known as the E_{Rigid}, the energy released on Cu (111) and Al (111) is known as the E_{Def} [34]. Figures 5 depict the two perspectives of adsorbed compound A on the Cu (111) surface, whereas Figures 6 display the perspectives of compounds on the Al (111) surface. On Cu (111) and Al (111), every molecule showed high surface coverage. The compounds are arranged parallel on Cu (111) and Al (111) via covalent and non-bonded contacts, supporting the low ΔE, E_{LUMO}, I, and η and high E_{HOMO}, A, σ, and ΔN values from DFT calculation (Tables 2 and 3), which suggests that the inhibitors accept electrons via back donation [17,35-36].

**Table 2**. Monte Carlo simulation outcome for inhibitor - Al (111) interaction

Compound (Al)	dE_{ad}/dN_i	Adsorption energy	Rigid adsorption energy	Deformation energy	Total energy
A	-283.49	-283.49	-18.340	-265.15	-6.65
B	-78.48	-157.82	-55.50	-102.32	-28.79
C	-14182	-14182	-25.025	-1393	-5.050

Compound	Side View	Top View

Compound A

Compound B
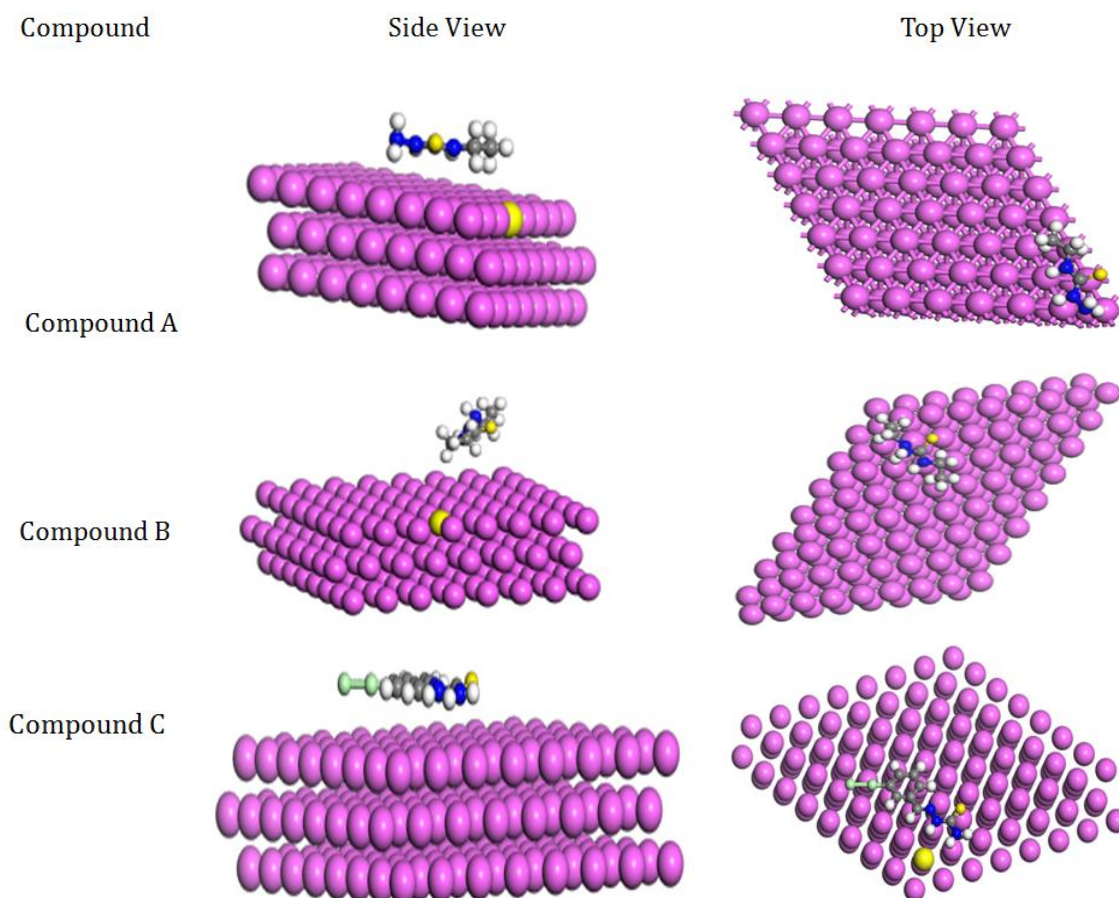
Compound C

Figure 5. Side view (left) and top view (right) of the thiosemicarbazide derivatives (compounds A-C) on the Al (111) surface.

Table 3. Monte Carlo simulation outcome for inhibitor - Cu (111) interaction

Compound (Cu)	dEad/dNi	Adsorption energy	Rigid adsorption energy	Deformation energy	Total energy
A	-271.99	-537.91	-6.139	-531.77	15.77
B	-62.96	-119.15	-8.090	-111.06	20.50
C	-14078	-28049	-12.53	-27923	21.35
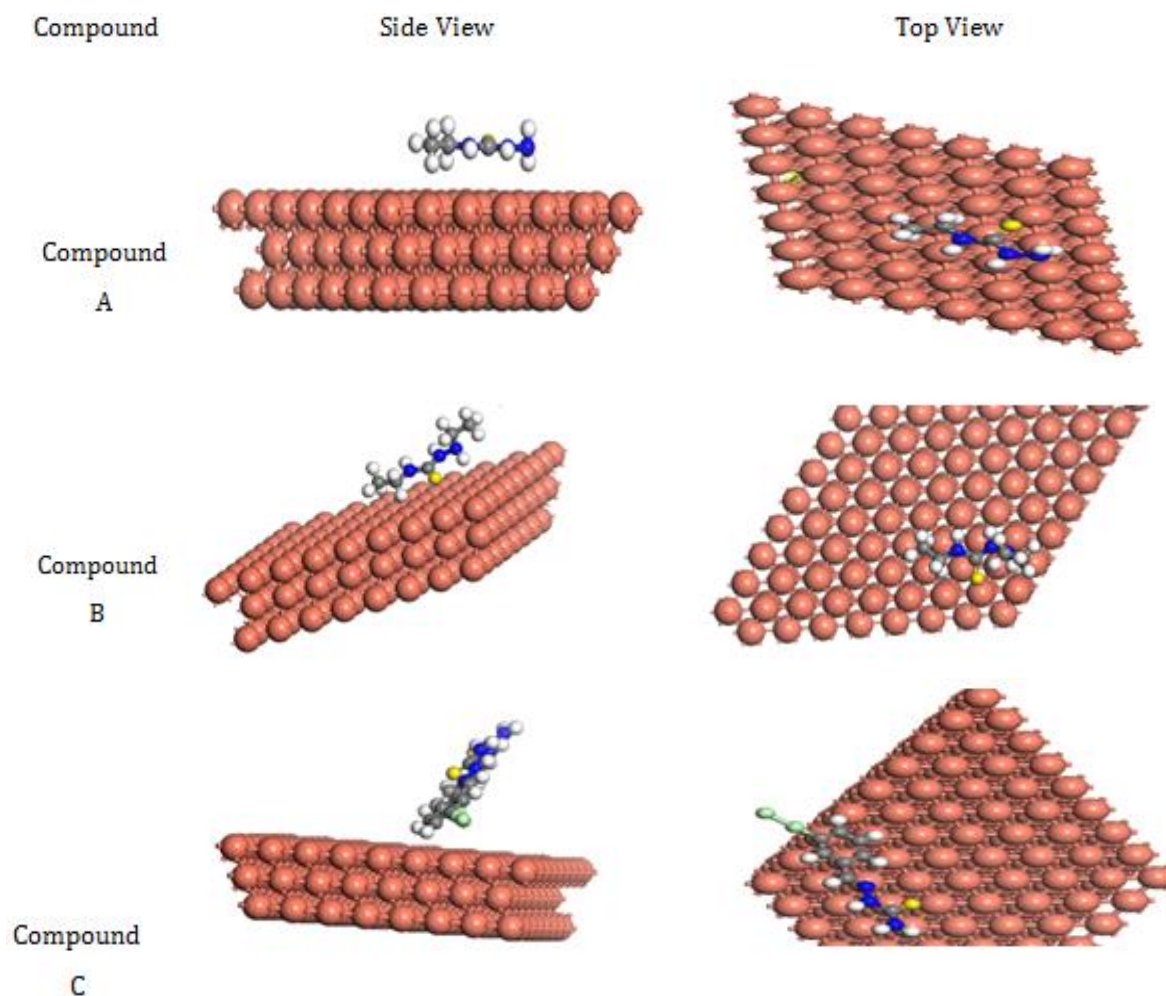
Figure 6. Side view (left) and top view (right) of the thiosemicarbazide derivatives (compounds A-C) on the Cu (111) surface.

Conclusion

In an acidic environment, the inhibitory effects of three thiosemicarbazide derivatives have been assessed theoretically against copper and aluminum surface corrosion. To display their inherent characteristics and reactivities, density functional theory (DFT) computations were performed. Monte Carlo simulation was employed to explain various likely interactions, including electrostatic and van der Waals interactions between the Cu (111) and Al (111) surfaces and the inhibitors. The findings lead to the following deductions:

1. The inconsistent distribution of charge was shown by the HOMO and LUMO maps.
2. The compounds showed high E_{HOMO}, A, σ, and ΔN, and low ΔE, E_{LUMO}, I, and η.
3. The electrostatic potential (ESP) map identified sites that donate electrons to empty d-orbitals of the metal and accept electrons from the metals via back donation.
4. The inhibitor three thiosemicarbazide derivatives have strong interactions with the Cu (111) and Al (111) surface, according to Monte Carlo simulations.
5. To assess how well the three compounds inhibit Cu (111) and Al (111) surface corrosion, a combination of the adsorption energy (E_{ads}) and the desorption energy (dE_{ads}/dN_i) values is used.
6. DFT and Monte Carlo simulations showed that these inhibitors are more effective in the following order: Compound C > Compound A > Compound B.

Disclosure Statement

No potential conflict of interest was reported by the authors.

Orcid

Terngu Timothy Uzah : 0000-0003-35562049

References

[1]. Li M., Ouyang Y., Yang W., Chen Y., Zhang K., Zuo Z., Yin X., Liu Y. Inhibition performances of imidazole derivatives with increasing fluorine atom contents in anions against carbon steel corrosion in 1 M HCl, *Journal of Molecular Liquids*, 2021, **322**:114535 [Crossref], [Google Scholar], [Publisher]

[2]. Dagdag O., Haldhar R., Kim S.C., Guo L., Gouri M.E., Berdimurodov E., Hamed O., Jodeh S., Akpan E.D., Ebenso E.E. Recent progress in epoxy resins as corrosion inhibitors: design and performance, *Journal of Adhesion Science and Technology*, 2023, **37**:923 [Crossref], [Google Scholar], [Publisher]

[3]. Dagdag O., El Harfi A., El Gana L., S Safi Z., Guo L., Berisha A., Verma C., Ebenso E.E., Wazzan N., El Gouri M. Designing of phosphorous based highly functional dendrimeric macromolecular resin as an effective coating material for carbon steel in NaCl: Computational and experimental studies, *Journal of Applied Polymer Science*, 2021, **138**:49673 [Crossref], [Google Scholar], [Publisher]

[4]. Conradi S. Development of mechanical, corrosion resistance, and antibacterial properties of steels, *Materials*, 2021, **14**:7698 [Crossref], [Google Scholar], [Publisher]

[5]. Odewole O.A., Ibeji C.U., Oluwasola H.O., Oyeneyin O.E., Akpomie K.G., Ugwu C.M., Ugwu C.G., Bakare T.E. Synthesis and anti-corrosive potential of Schiff bases derived 4-nitrocinnamaldehyde for mild steel in HCl medium: Experimental and DFT studies, *Journal of Molecular Structure*, 2021, **1223**:129214 [Crossref], [Google Scholar], [Publisher]

[6]. Oyeneyin O.E., Ojo N.D., Ipinloju N., James A.C., Agbaffa E.B. Investigation of corrosion inhibition potentials of some aminopyridine schiff bases using density functional theory and Monte Carlo simulation, *Chemistry Africa*, 2022, **5**:319 [Crossref], [Google Scholar], [Publisher]

[7]. Ibrahim M.A., Moussa N.A., Mahmoud A.H., Sayed S.R., Sidhom P.A., Abd El-Rahman M.K., Shoeib T., Mohamed L.A. Density functional theory study of the corrosion inhibition performance of 6-mercaptopurine and 6-thioguanine expired drugs toward the aluminium (111) surface, *RSC advances*, 2023, **13**:29023 [Crossref], [Google Scholar], [Publisher]

[8]. Verma C., Ebenso E.E., Quraishi M., Hussain C.M. Recent developments in sustainable corrosion inhibitors: design, performance and industrial scale applications, *Materials Advances*, 2021, **2**:3806 [Crossref], [Google Scholar], [Publisher]

[9]. Ihamdane R., Tiskar M., Outemsaa B., Zelmat L., Dagdag O., Berisha A., Berdimurodov, E., Ebenso E.E., Chaouch A. Essential oil of Origanum vulgare as a green corrosion inhibitor for carbon steel in acidic medium, *Arabian Journal for Science and Engineering*, 2023, **48**:7685 [Crossref], [Google Scholar], [Publisher]

[10]. Shanaghi A.L.I. Chu P.K., Moradi, H. Effect of inhibitor agents addition on corrosion resistance performance of titania sol–gel coatings applied on 304 stainless steel. *Surface Review and Letters*, 2017, **24**:1750055 [Crossref], [Google Scholar], [Publisher]

[11]. Al-Amiery A., Kadhim A., Al-Adili A., Tawfiq Z. Limits and developments in ecofriendly corrosion inhibitors of mild steel: a critical review. Part 1: Coumarins, *International Journal of Corrosion and Scale Inhibition*, 2021, **10**:1355 [Crossref], [Google Scholar]

[12]. Ogunyemi B., Ojo F. Corrosion inhibition potential of thiosemicarbazide derivatives on aluminium: Insight from Molecular Modelling and QSARS approaches, *Journal of the Nigerian Society of Physical Sciences*, 2023, **5**:915 [Crossref], [Google Scholar], [Publisher]

[13]. Acharya P.T., Bhavsar Z.A., Jethava D.J., Patel D.B., Patel H.D. A review on development of bio-active thiosemicarbazide derivatives: Recent advances, *Journal of Molecular Structure*, 2021, **1226**:129268 [Crossref], [Google Scholar], [Publisher]

[14]. Gummanar N., Mokshanatha P.B., Dyapur P., Yallappa G.N. Organic corrosion inhibitors for aluminumbased alloys–A review, *Letters in Applied NanoBioScience*, 2023, **12**:170 [Crossref], [Google Scholar]

[15]. Kaplancıklı Z.A., Altıntop M.D., Sever B., Cantürk Z., Özdemir A. Synthesis and in vitro evaluation of new thiosemicarbazone derivatives as potential antimicrobial agents, *Journal of Chemistry*, 2016, **2016**[Crossref], [Google Scholar], [Publisher]

[16]. Verma D.K., Aslam R., Aslam J., Quraishi M., Ebenso E.E., Verma C. Computational modeling: theoretical predictive tools for designing of potential organic corrosion inhibitors, *Journal of Molecular Structure*, 2021, **1236**:130294 [Crossref], [Google Scholar], [Publisher]

[17]. Akbari Z., Stagno C., Iraci N., Efferth T., Omer E.A., Piperno A., Montazerozohori M., Feizi-Dehnayebi M., Micale N. Biological evaluation, DFT, MEP, HOMO-LUMO analysis and ensemble docking studies of Zn (II) complexes of bidentate and tetradentate Schiff base ligands as antileukemia agents, *Journal of Molecular Structure*, 2024, **1301**:137400 [Crossref], [Google Scholar], [Publisher]

[18]. Uzah T.T., Mbonu I.J., Gber T.E., Louis H. Synergistic effect of KI and urea on the corrosion protection of mild steel in 0.5 M H2SO4: Experimental and computational insights, *Results in Chemistry*, 2023, **5**:100981 [Crossref], [Google Scholar], [Publisher]

[19]. Iorhunaa F., Nyijime A.T., Lawal S.M. Theoretical properties of thiazepine and its derivatives on inhibition of aluminium Al (110) surface, *Algerian Journal of Engineering and Technology*, 2023, **8**:43 [Google Scholar], [Publisher]

[20]. Esmaeilzadeh Khabazi M., Najafi Chermahini A. DFT study on corrosion inhibition by tetrazole derivatives: investigation of the substitution effect, *ACS Omega*, 2023, **8**:9978 [Crossref], [Google Scholar], [Publisher]

[21]. Guo L., Obot I.B., Zheng X., Shen X., Qiang Y., Kaya S., Kaya C. Theoretical insight into an empirical rule about organic corrosion inhibitors containing nitrogen, oxygen, and sulfur atoms, *Applied Surface Science*, 2017, **406**:301 [Crossref], [Google Scholar], [Publisher]

[22]. Fouda A., Etaiw S., Ibrahim A., El-Hossiany A. Insights into the use of two novel supramolecular compounds as corrosion inhibitors for stainless steel in a chloride environment: experimental as well as theoretical investigation, *RSC Advances*, 2023, **13**:35305 [Crossref], [Google Scholar], [Publisher]

[23]. Oukhrib R., Abdellaoui Y., Berisha A., Abou Oualid H., Halili J., Jusufi K., Ait El Had M., Bourzi H., El Issami S., Asmary F.A. DFT, Monte Carlo and molecular dynamics simulations for the prediction of corrosion inhibition efficiency of novel pyrazolylnucleosides on Cu (111) surface in acidic media, *Scientific Reports*, 2021, **11**:3771 [Crossref], [Google Scholar], [Publisher]

[24]. Simonović A.T., Tasić Z.a.Z., Radovanović M.B., Petrović Mihajlović M.B., Antonijević M.M. Influence of 5-chlorobenzotriazole on inhibition of copper corrosion in acid rain solution, *ACS Omega*, 2020, **5**:12832 [Crossref], [Google Scholar], [Publisher]

[25]. Nyijime T.A., Chahul H.F., Ayuba A., Iorhuna F. Theoretical investigations on thiadiazole derivatives as corrosion inhibitors on mild steel, *Advanced Journal of Chemistry section A*, 2023, **6**:141 [Crossref], [Google Scholar], [Publisher]

[26]. Hadisaputra S., Purwoko A.A., Hakim A., Prasetyo N., Hamdiani S. Corrosion Inhibition Properties of Phenyl Phthalimide Derivatives against Carbon Steel in the Acidic Medium: DFT, MP2, and Monte Carlo Simulation Studies, *ACS Omega*, 2022, **7**:33054 [Crossref], [Google Scholar], [Publisher]

[27]. Datta D. Geometric mean principle for hardness eualization: a corollary of Sanderson's geometric mean principle of electronegativity equalization, *The Journal of Physical Chemistry*, 1986, **90**:4216 [Crossref], [Google Scholar], [Publisher]

[28]. Kaya S., Kaya C. A new method for calculation of molecular hardness: a theoretical study, *Computational and Theoretical Chemistry*, 2015, **1060**:66 [Crossref], [Google Scholar], [Publisher]

[29]. Iorhuna F., Thomas N.A., Lawal S.M. A Theoretical properties of Thiazepine and its derivatives on inhibition of Aluminium Al (110) surface, *Algerian Journal of Engineering and Technology*, 2023, **8**:43 [Crossref], [Google Scholar]

[30]. Jabri Z., El Ibrahimi B., Jarmoni K., Sabir S., Misbahi K., Rodi Y.K., Mashrai A., Hökelek T., Mague J.T., Sebbar N.K., New imidazo [4, 5-B] pyridine derivatives: synthesis, Crystal strustures, hirshfeld surface analysis, DFT Computations and monte carlo simulations, *Journal of Chemical Technology & Metallurgy*, 2022, **57**:451 [Google Scholar]

[31]. Arrousse N., Fernine Y., Al-Zaqri N., Boshaala A., Ech-chihbi E., Salim R., El Hajjaji F., Alami A., Touhamie M.E., Taleba M., Thiophene derivatives as corrosion inhibitors for 2024-T3 aluminum alloy in hydrochloric acid medium, *RSC Advances*, 2022, **12**:10321 [Crossref], [Google Scholar], [Publisher]

[32]. Thakur A., Kumar A. Computational insights into the corrosion inhibition potential of some pyridine derivatives: A DFT approach, *European Journal of Chemistry*, 2023, **14**:246 [Crossref], [Google Scholar], [Publisher]

[33]. Uzah T.T., Mbonu I.J. Insight into synergistic corrosion inhibition of thiourea and ZnCl2 on mild steel: Experimental and theoretical Approaches, *Journal of Chemistry Letters*, 2024, **4**:211 [Google Scholar]

[34]. Esmaeilzadeh Khabazi M., Najafi Chermahini A. DFT study on corrosion inhibition by tetrazole derivatives: investigation of the substitution effect, *ACS Omega*, 2023, **8**:9978 [Crossref], [Google Scholar], [Publisher]

[35]. Nduma R.C., Fayomi O.S.I., Nkiko M.O., Inegbenebor A.O., Udoye N.E., Onyisi O., Sanni O., Fayomi J. Review of metal protection techniques and application of drugs as corrosion inhibitors on metals, *IOP Conference Series: Materials Science and Engineering*, 2021, **1107**:012023 [Google Scholar],

[36]. Benzidia B., Barbouchi M., Hsissou R., Zouarhi M., Erramli H., Hajjaji N. A combined experimental and theoretical study of green corrosion inhibition of bronze B66 in 3% NaCl solution by Aloe saponaria (syn. Aloe maculata) tannin extract, *Current Research in Green and Sustainable Chemistry*, 2022, **5**:100299 [Crossref], [Google Scholar], [Publisher]